Extraction Kinetics and Physicochemical Studies of *Terminalia catappa* L Kernel Oil Utilization Potential

Menkiti, Matthew*[*+]

Civil and Environmental Engineering Department, Water Resources Center, Texas Tech. University, Lubbock, Texas, USA

Agu, Chinedu M.

Chemical Engineering Department, Nnamdi Azikiwe University, Awka, NIGERIA

Agu, Ijeoma E.

Civil Engineering Department, University of Nigeria, Nsukka, NIGERIA

ABSTRACT: *Kinetics and selected variables (temperature, particle size and time) for extraction of Terminalia Catappa L Kernel Oil (TCKO) were investigated using solvent extraction. Kinetic models studied were: parabolic diffusion, power law, hyperbolic, Elovich and pseudo second order. In ascending order, the best- fitted models at the optimum temperature and oil yield were Elovich's model, hyperbolic model, and Pseudo second order model. Due to highest value of linear correlation coefficient (R^2) and lowest average values of Root Mean Square (RMS), absolute relative deviation (AARD %) and Standard Error of Estimation (SEE) recorded for Pseudo second order, it was selected as the best fit model. Parabolic and power law models failed to give good fit. The average maximum oil yield of 60.45 ± 0.05 % was obtained at temperature of 55 °C, time of 150 min and an average particle size of 0.5 mm. The physicochemical properties of the TCKO showed its potential for industrial applications.*

KEYWORDS: *Kinetics; Solvent extraction; Terminalia catappa L.*

INTRODUCTION

There have been growing interests in the study of the extraction of vegetable oils from its natural sources (seeds, nuts, leaves). The reason for this is that such oil resources are not limited to their sole utilization as precursor for edible vegetable oil production, but also as potential base-stock for numerous machine oils such as lubes [1 – 2], types of diesel [3 – 4], biodiesels [5 – 7] and

transformer oil [8], which is the focus of this study. The biodegradability of vegetable oil offers a major environmental advantage over its petroleum oil base counterpart, which is currently widely in use, though not in all specific cases [9 – 10].

In light of this, there is a need to study oil (triglycerides) extraction routes (with emphases on

kinetics and process variables in this report) from seeds and nuts in order to make an informed choice of any of the methods, prior to its potential application for both industrial and domestic purposes. These routes include but not limited to solvent, supercritical fluid, sonication-assisted, microwave-assisted, accelerated solvent extraction methods that could be used in the extraction of oil from seeds, nuts, and leaves [11].

Among these methods, solvent extraction, which is the most commonly used provides the focus for this study. Its major advantage is relative simplicity and cost effectiveness [12 – 13] in the removal of a soluble fraction (known as the solute) from an insoluble solid [14-16]. In oil extraction industry, n-hexane is most commonly used as the extracting solvent. This could be attributed to its extraction potential, nonpolar property (zero polarity index), low boiling point as well as its cost [17-18].

Over the years, solvent extraction has been used in the extraction of oil from a number of seeds and nuts, including *Jatropha curcas* [19], grape seed [20], coconut [21], soyabean [22] and *Terminalia catappa* [9].

However, this work is focused on oil extraction from *Terminalia catappa* (Tropical Almond) using a solvent extraction method with n-hexane as the solvent. *Terminalia Catappa* (TC) tree belongs to the Combretaceae family. It is native to Meridional Asia and thrives in well-aerated and drained sandy soils and often grown for ornamental purposes [4, 23]. Over time, most researches on TC have covered the biological and phytochemical properties of the bark, leaves, and fruit extracts for medicinal purposes, with insignificant attention on the large-scale oil extraction from its kernels or its potential for other uses [24 – 28]. The *Terminalia Catappa* Kernel (TCK) (583.0 g/kg dry matter) oil quantity is similar to that of sunflower, peanut, and rapeseed [29]. TC kernels purportedly contain high amount of oil: 63.65 % [23], 60.45 % [30], 60 % [31], 50 % [3] and 49 % [4] which justifies its potential applications for industrial purposes.

In this report, extraction process parameters such solvent type, extraction temperature, particle size of the solute sample, solute to solvent ratio were investigated as a complement to the extraction process kinetics [12-13]. Several kinetic models have been previously applied to describe solvent extraction by a number of researchers. For instance, *Kitanovic et al,* [16] used parabolic diffusion, power law, hyperbolic, Weibull's and Elovich's models to describe the extraction of resinoid from aerial parts of St John's Wort (Hypericum Perforatum L.). *Qu et al.* [32] used a second order model in describing the extraction of antioxidants from pomegranate marc. Like numerous earlier and current studies, extraction kinetics, thermodynamics and biodegradability of the extracted oil (TCKO in this case) would be vital in evaluating whether to apply the extracted oil and process industrially [16]. Meanwhile, the current study focuses on the linear extraction kinetics of TCKO with respect to its potential utilization for transformer fluid production. Furthermore, considering the relatively high volume of oil yield from TCK, it is imperative to investigate specified extraction kinetic models in order to determine the model that would adequately govern the extraction process, particularly for application of TCKO as a commercial feed-stock for transformer fluid production.

This report, therefore, aims to investigate the kinetics of TCKO extraction at different operating conditions using parabolic diffusion, power law, hyperbolic, Elovich's and pseudo second order models. In order to evaluate its suitability as base fluid for transformer oil, the physicochemical properties of the extracted TCKO were determined, while Fourier Transform InfraRed (FT-IR) was also applied to determine the predominate functional groups existing in the TCKO.

EXPERIMENTAL SECTION
Materials

The materials used include *Terminalia catappa* L. kernels, n-hexane solvent, Soxhlet Extractor, siphon tube, round bottom flask, thermometer, electrical blender, sieves of different sizes, rotary vacuum evaporator. The *Terminalia catappa* L. kernels were harvested by hand picking during the dry season, from the south eastern part of Nigeria. The kernels obtained were oven dried at 60 °C for 12 h. prior to its hand-milling [18]. The milled TC kernels were sieved into various particle sizes of 0.5 mm, 1.0 mm, 1.5 mm, 2.0 mm and 2.5 mm using 5 standard sieves.

N-Hexane (99 % purity level) used was purchased from laboratory chemical vendors in Ogbete market, Enugu, Nigeria.

Method of oil extraction

20 g of milled TC kernel and 200 ml of n-hexane were placed in a Soxhlet Extractor and heated for

150 min at 55 °C. Oil extraction was carried out using Soxhlet Extractor according to the procedure described by *Menkiti et al.* [18]. The oil extract leached through the pores of the thimble of the extractor into the siphon tube. It then flowed down into the round bottom flask. The kernel residue was washed with 20 ml of n-hexane for 20 min. The oil extract was then dried under vacuum at 60 °C until a constant weight was obtained. The percentage oil yield of TC kernel obtained at these conditions was calculated using equation 1.

For the temperature study, 20 g milled TC kernel and 200 mL n-hexane were placed in Soxhlet Extractor connected to a condenser. The ratio of the TC kernels (solute) and n-hexane (solvent) was 1:10g/ml. A series of five Soxhlet Extractors were placed in a thermostatic bath at different temperatures (35, 40, 45, 50, 55 °C). The extraction was performed at different time intervals of 30, 60, 90, 120 and 150 min for each temperature. The whole extraction process performed under every set of conditions was done three times. Thereafter, the average values were reported, while the total extraction yield was obtained using the procedure described by *Menkiti et al.* [18]. At the end of every extraction cycle, the oil yield obtained was calculated using Equation (1). The residual solvent was evaporated using a rotary vacuum evaporator at 60 °C.

$$\% \text{Oil yield} = \frac{\text{weight of oil extracted}(g)}{\text{weight of TC ker nel}(g)} \times 100 \qquad (1)$$

Statistical method for extraction kinetic models

Kinetic model parameters were calculated from their linearized forms (Table 1). The tools for estimating the models that best represented the experimental data were magnitudes of the linear correlation coefficient (R^2), the root mean square (RMS), the Average Absolute Relative Deviation (AARD %) [33] and the Standard Error of Estimation (SEE) [34]. The RMS, AARD and SEE were calculated using equations 2, 3 and 4, respectively.

$$\text{RMS} = \sqrt{\frac{1}{N}\sum_{i=1}^{N}\left(\frac{q_{exp} - q_{cal}}{q_{exp}}\right)^2} \qquad (2)$$

$$\text{AARD} = \frac{1}{N}\sum_{i=1}^{N}\left|\frac{q_{exp} - q_{cal}}{q_{exp}}\right| \times 100 \qquad (3)$$

$$\text{SEE} = \sqrt{\frac{\sum(x - y)^2}{dt}} \qquad (4)$$

Where N is the number of experimental data points. q_{cal} and q_{exp} are the calculated and experimental values, respectively, in Equations (2) and (3), while x and y are experimental and calculated values in Equation (4). The dt is the change in time.

The higher the value of the linear correlation coefficient R^2 and the lower the values of the RMS, AARD and SEE, the better will be the goodness of fit [16, 30].

Fourier Transform InfraRed (FT-IR) spectroscopy analysis

The FT-IR analysis of the oil samples was carried out using BUCK Scientific Infrared Spectrophotometer Model 530.

RESULTS AND DISCUSSION
Temporal yield profile for TCK at varying conditions, kinetic parameters, and kinetic models studies

Observations from Figs. 1-5 show two distinct extraction regimes that depicted the extraction process. These regimes are: the fast washing action that occurred at the beginning (between 30 and 90 min) and a slow diffusion controlled extraction that follows later (between 90 and 150 min) [16, 30]. Owing to the high rate of fast washing, the first regime is not easily noticeable. Figs. 1 – 5 indicate that for the different particle sizes at 35, 40, 45, 50, and 55 °C, the time dependent yields are parabolic-like. It has a high initial slope and subsequently exponential shape, corresponding to slow washing and fast diffusion regimes, respectively. This is in line with most solid-liquid extraction curves [16, 21, 30].

It is evident from Figs. 1 to 5 that oil yield increased with temperature during the extraction process. This was as a result of the increase in diffusion (as oil molecules acquire more kinetic energy) of the oil and decrease in viscosity as the temperature increased [21, 35-36]. Temperature increase would also enhance the mass transfer coefficient of extraction and thus improve the extraction yield [18, 21, 37 – 38]. Figs. 1 to 5 show increase in oil yield with decrease in the average particle size. This could be attributed to the bigger interfacial area of the solid as the particle size increased. It implies that

Table 1: Models names and descriptive non-linear and linearized equations.

Kinetic models	Non-linear equations	Linearized equations
Parabolic diffusion	$\bar{q} = A_0 + A_1 t^{1/2}$	$\bar{q} = A_0 + A_1 t^{1/2}$
Power law	$\bar{q} = B t^n$	$Ln\bar{q} = LnB + nLnt$
Hyperbolic	$\bar{q} = \dfrac{C_1 t}{1 + C_2 t}$	$\dfrac{1}{\bar{q}} = \dfrac{1}{C_1} \times \dfrac{1}{t} + \dfrac{C_2}{C_1}$
Elovich's	$\bar{q} = E_0 + E_1 \ln t$	$\bar{q} = E_0 + E_1 \ln t$
Pseudo second order	$\bar{q} = \dfrac{C_s^2 kt}{1 + C_s kt}$	$\dfrac{t}{C_t} = \dfrac{t}{kC_s^2} + \dfrac{t}{C_s}$

A_0, A_1 parabolic diffusion model parameters: washing coefficient (1) and diffusion rate constant (min$^{-0.5}$), respectively.
B power law parameter incorporating the characteristics of the extraction system (min^{-n}).
C_1, C_2 hyperbolic model parameter: extraction rate at the beginning (min^{-1}) and constant related to maximum extraction yield (min^{-1}), respectively.
C_s, C_t Pseudo second order model parameter: equilibrium concentration of oil (g/L) in the extract and concentration of oil (g/L) in the suspension
E_0, E_1 Elovich equation parameters (L).
k extraction rate constant.
n diffusional exponent of the power law model (L).
q extraction yield.
t time (min)
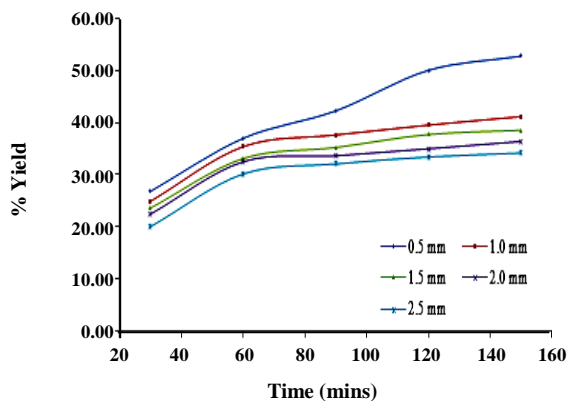
Fig. 1: Temporal extraction yield profile for TC kernel at temp. of 35°C.

Fig. 2: Temporal extraction yield profile for TC kernel at temp. of 40°C.

intra-particle diffusion resistance becomes smaller for small particle sizes due to the shortened diffusion path. Hence, the reason why smaller kernel particles had higher final yields were attributed to the increased surface area of the smaller milled samples with declining particle size. This leads to high rate of oil dissolution from the smaller samples into the solvent, as well as increased mass transfer rate that is attributed to shortened diffusion path [18, 39 – 40]. On the other hand, intra-particle diffusion effect would be more pronounced for bigger particles leading to appreciable decrease in oil extraction. In this

situation, some of the oil would not be extracted due to minimal contact surface area, difficulty of solvent entrainment and limited diffusion of oil from the internals of the larger particle to the solvent [21, 41-42]. However, the rate of extraction would increase, with finer grinding, since more oil would be freed from the cells, as demonstrated in Figs 1 to 5.

Table 2 summarizes the kinetic parameter of the hyperbolic, Elovich's and pseudo second order kinetic models studied at 50 °C and 55 °C. On the other hand, Table S1 shows the kinetic parameters of the entire
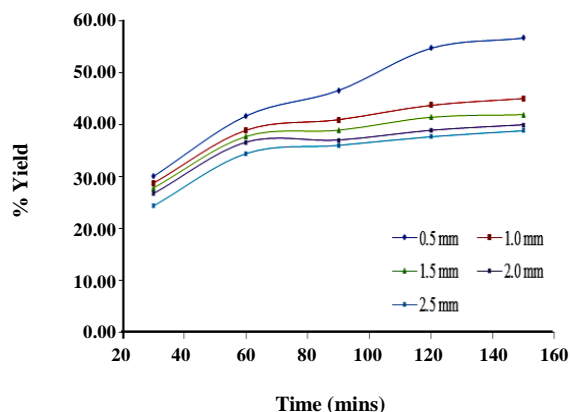
Fig. 3: Temporal extraction yield profile for TC kernel at temp. of 45°C.
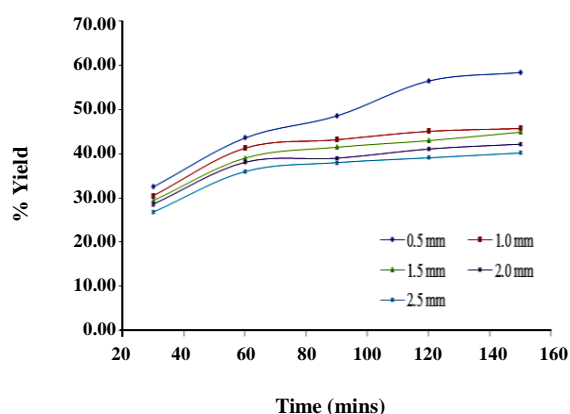
Fig. 4: Temporal extraction yield profile for TC kernel at temp. of 50°C.
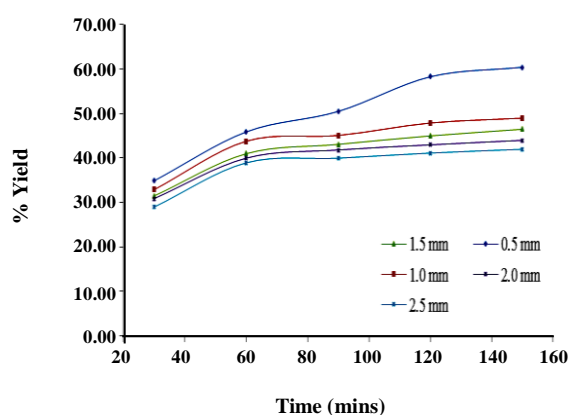
Fig. 5: Temporal extraction yield profile for TC kernel at temp. of 55°C.

studied models at temperatures 35 °C, 40 °C, 45 °C 50 °C and 55 °C. The parameters C_1 and C_2 for the hyperbolic model both increased with increase in temperature across the entire five particle sizes. It was also observed from Table 2 that majority of the kinetic parameters E_0, E_1 and K, C_s for Elovich's and pseudo second order models respectively, increased with temperature across the five different particle sizes. The consistent increase in parameter values of these models is associated with increases in oil yields values observed with temperature increases. Hence, the insignificant difference observed between the models' calculated oil yields and that of the experimental oil yield value [18, 43]. A similar result was observed by *Kitanovic et al.* [16] for the solvent extraction of resinoid from aerial part of *Hypericum perforatum* L using different solute to solvent ratios. From Table 2, it could be seen that there was greater consistent increase in the values of parameters C_2, E_0 and K for hyperbolic, Elovich's and pseudo second order models, respectively, as the particle sizes increased from 0.5 mm to 2.5 mm for the two different temperatures (50 °C and 55 °C). Furthermore, there was also greater consistent decrease in the parameter values C_1, E_1 and C_S for hyperbolic, Elovich's and pseudo second order models, respectively, as the particle size increased. The consistent increase of the kinetic parameters values for hyperbolic, Elovich's and pseudo second order models with temperature is attributed to the predominance of diffusion rate over the washing mechanism process, hence, ensures greater/higher oil yield in these models [18, 43].

On the contrary, there was the high inconsistent trend for the kinetic parameter values obtained for parabolic and power law models (see supplementary data, Table S1). From Table S1, it could be seen that only some of the parameters A_0 and B increased with increase in temperature while, the kinetic parameters A_1 and *n* did not have a definite trend with temperature increase as could be observed in Table S1. This consistent increase in parameter values of these models indicates that in these models, oil yield does not always increase with temperature increase. Hence, there is predominance of washing mechanism, over the rate of oil diffusion. This is evident in the significant difference between the models' oil yield and the experimentally obtained oil yield [43].

Table 2: Linearized Kinetic parameters for TC oil extraction at 50 and 55 °C for hyperbolic, Elovich's and pseudo second order models.

	50°C					55°C				
	0.5mm	1.0mm	1.5mm	2.0mm	2.5mm	0.5mm	1.0mm	1.5mm	2.0mm	2.5mm
Hyperbolic										
C_1	1.969	2.413	2.301	2.392	2.138	2.234	2.690	2.632	2.762	2.488
C_2	0.028	0.045	0.044	0.049	0.045	0.031	0.048	0.049	0.055	0.051
R^2	0.988	0.975	0.989	0.973	0.978	0.985	0.979	0.989	0.979	0.958
RMS (%)	0.028	0.026	0.017	0.024	0.024	0.028	0.022	0.016	0.020	0.030
SEE	0.585	0.441	0.281	0.378	0.357	0.621	0.398	0.262	0.331	0.480
ARE %	0.113	0.150	0.163	0.069	0.207	0.174	0.071	0.136	0.168	0.184
SSE	10.26	5.83	2.37	4.28	3.82	11.55	4.76	2.07	3.29	6.92
HYBRID %	0.19	0.25	0.27	0.11	0.35	0.29	0.12	0.23	0.28	0.31
MPSED %	3.56	3.32	2.24	3.14	3.08	3.64	2.87	2.01	2.59	3.89
SD	0.0023	0.0045	0.0049	0.0021	0.0062	0.0035	0.0014	0.0041	0.0050	0.0055
Elovich's										
E_0	-23.702	0.338	-1.177	2.229	0.506	-20.098	1.196	1.776	5.230	4.178
E_1	16.434	9.368	9.349	8.162	8.149	16.085	9.761	9.095	7.966	7.810
R^2	0.988	0.919	0.956	0.924	0.925	0.988	0.937	0.954	0.922	0.882
RMS (%)	0.020	0.041	0.031	0.037	0.039	0.019	0.035	0.029	0.035	0.045
SEE	0.417	0.647	0.466	0.543	0.539	0.417	0.589	0.461	0.539	0.665
ARE %	0.007	0.227	0.146	0.193	0.211	0.017	0.171	0.125	0.157	0.258
SSE	5.229	12.554	6.523	8.843	8.727	5.207	10.401	6.369	8.727	13.257
HYBRID %	0.011	0.378	0.243	0.322	0.352	0.029	0.284	0.208	0.261	0.429
MPSED %	2.583	5.321	4.028	4.834	5.070	2.510	4.542	3.776	4.517	5.825
SD	0.000	0.007	0.004	0.006	0.006	0.001	0.005	0.004	0.005	0.008
2nd order										
C_s	74.63	51.81	51.02	47.17	45.25	75.19	55.25	52.08	48.54	46.51
K	3.2×10^{-4}	1.1×10^{-3}	9.5×10^{-4}	1.2×10^{-3}	1.2×10^{-3}	3.5×10^{-4}	9.7×10^{-4}	1.0×10^{-3}	1.4×10^{-3}	1.4×10^{-3}
R^2	0.993	0.998	0.999	0.998	0.998	0.994	0.998	0.999	0.999	0.998
RMS (%)	0.030	0.031	0.019	0.026	0.028	0.031	0.024	0.017	0.024	0.036
SEE	0.545	0.434	0.268	0.370	0.351	0.579	0.389	0.257	0.339	0.484
ARE %	0.031	0.460	0.290	0.128	0.229	0.162	0.211	0.028	0.092	0.364
SSE	8.904	5.664	2.148	4.109	3.686	10.068	4.533	1.980	3.454	7.035
HYBRID %	0.051	0.767	0.484	0.213	0.382	0.270	0.351	0.047	0.153	0.607
MPSED %	3.861	3.975	2.411	3.401	3.624	4.008	3.089	2.164	3.084	4.636
SD	0.001	0.014	0.009	0.004	0.007	0.003	0.006	0.001	0.003	0.011

Research Article

Fig. 6(a to e) show the plots (histogram) that compares the experimental and calculated TCK oil yields using a pseudo second order model at different operation conditions. Similarly, Figs S1 to S4, compare the experimental and the calculated yields for the extraction of oil from TCK at different operating conditions for parabolic, power law, hyperbolic and Elovich's models, respectively. From Fig.6 (a to e), it would be observed that the experimental and the calculated oil yields values for the pseudo second order model were significantly close. For instance, in Fig. 6 (a) the values of the experimental and calculated oil yields at 55 °C, 0.5 mm particle size and 150 min, were 60.45 ± 0.05 % and 60.08 ± 0.05 % respectively. In this case, an insignificant difference of 0.37 ± 0.05 % was recorded for the pseudo second order model, thus indicating good fit for the model. This was due to the predominance of diffusion rate over the washing mechanism process, hence, ensures greater/higher oil yield that is comparable to the experimental yield [16, 43]. It could be observed from Figs. S1 (a to e) and S2 (a to e) for parabolic diffusion and power law models, respectively, that there were observable differences between the experimental and their respective calculated oil yields values. For instance, in Fig. S1 (a), the values of the experimental and calculated oil yields for parabolic diffusion model at 55 °C, 0.5 mm and 150 min, were 60.45 ± 0.05 % and 36.14 ± 0.05 %, respectively. The difference between the experimental and calculated value for the parabolic diffusion model was 24.31 ± 0.05 %. Similarly, in Fig. S2 (a), the values of the experimental and calculated oil yields for power law model at 55 °C, 0.5 mm and 150 min, were 60.45 ± 0.05 % and 89.43 ± 0.05 %, respectively. Like the parabolic diffusion model, the difference between the experimental and calculated yield values for power law model was 28.98 ± 0.05 %. These high % yield differences indicate that parabolic diffusion and power law models failed to give a good fit to the experimental data. This could be attributed to the slower diffusion mechanism than the washing mechanism, thus, lower oil yield when compared to the experimental yield [43]. Hence, could not be used to fit the extraction of oil from TCK under the studied extraction conditions.

From Figs. S3 (a to e) and S4 (a to e) for hyperbolic and Elovich's models, respectively, it would be observed that the experimental and the calculated oil yields values

for these models were significantly close. This was an indication of the good fit of the models to the experimental data. Such similar results, indicating good fit as was recorded for pseudo second order model, were also recorded for hyperbolic and Elovich's models.

Consequently, the significant difference between the % yield values for the experimental and calculated parabolic and power law models further justify the inconsistent trend of their kinetic parameters with a variation of temperature. On the other hand, the closeness between the % yield for the experimental and calculated for hyperbolic, Elovich's and pseudo second order models, justifies the relative consistent trend of their kinetic parameters with variation of process parameters.

Furthermore, R^2, RMS, AARD % and SEE were used adopted to estimate how well models represent the experimental data. In general, the higher the value of R^2 and lower the values of RMS, AARD % and SEE, the better would be the goodness of the model to fit the experimental data [16]. It could be seen from Table 2 that irrespective of the particle size and temperature used, individual values of the RMS were all less than 0.5 for each of the Hyperbolic, Elovich and Pseudo second order models. Similarly, individual values of the AARD % were less than 0.5 %, while those of SEE were all less than 0.7, for each of the Hyperbolic, Elovich and Pseudo second order models. Thus, based on their very low RSM, AARD % and SEE, these three models tested were considered adequate to model the extraction of oil from TCK.

On the other hand, for each of the parabolic diffusion and power law models, majority of their RMS values were less than 0.5. However, the individual values of AARD % for parabolic and power law models were much higher than 5 % while their SEE values were also relatively higher than those of Hyperbolic, Elovich's and pseudo second order models. Therefore, these two models (parabolic and power law models) tested were evaluated as not being good enough to model the extraction of oil from TCK as stated earlier. These results differ from the result obtained by *Kitanovic et al.* [16] for the resinoid extraction from aerial parts of *Hypericum perforatum L.*

On the basis of the values of the error analyses used, the best fit for the models increased in the following order:

Power law model $\rightarrow$ parabolic diffusion model $\rightarrow$ Elovich's model $\rightarrow$ Hyperbolic Model $\rightarrow$ Pseudo second order.
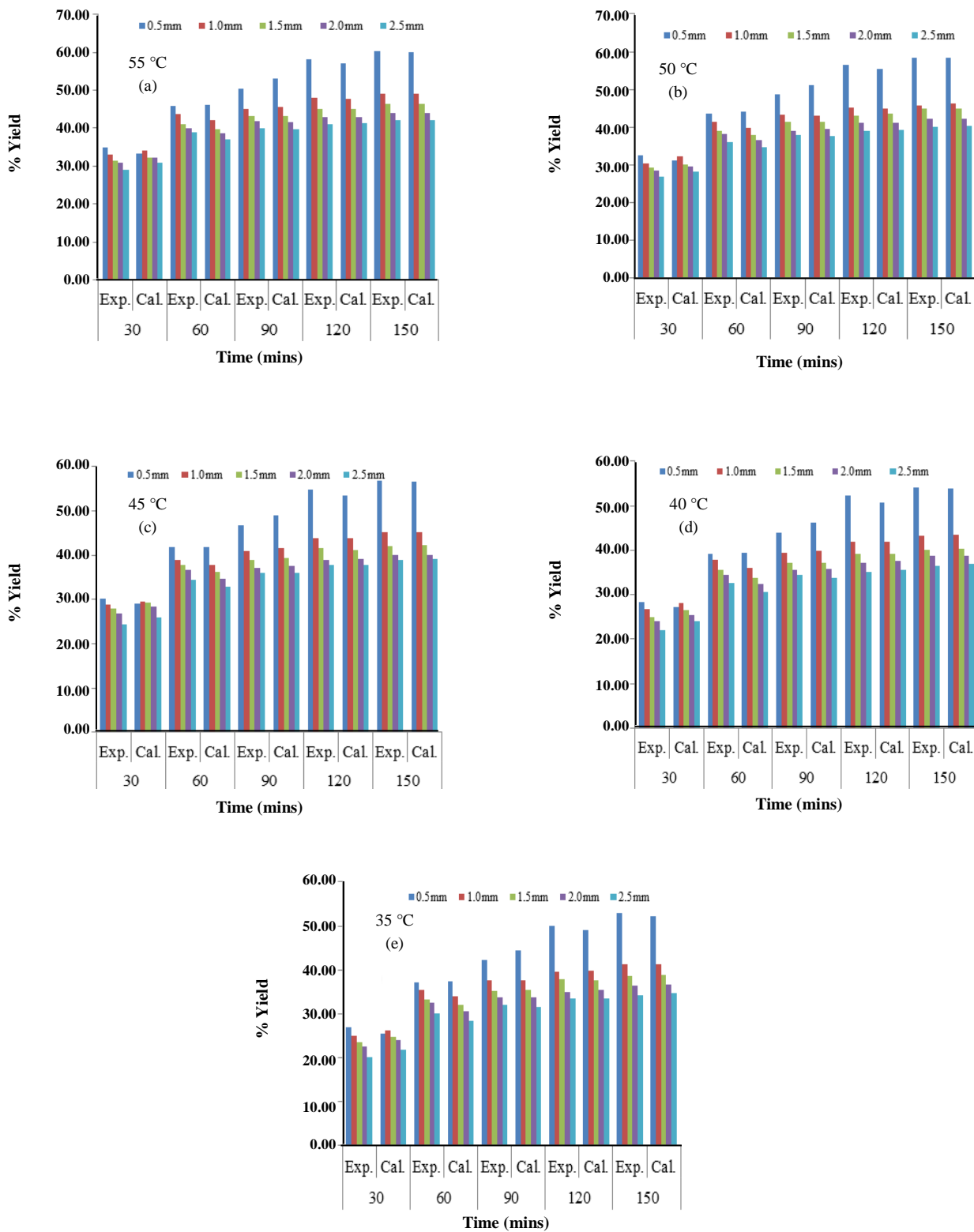
***Fig. 6a to e: Comparison of experimental and the calculated yields using pseudo second order model for TCK oil
extraction at different operation conditions.***

Table 3: Physicochemical properties of the TCKO.

Oil property	TCKO [a]	TCKO [b]	Standard Method
Oil yield (%) Dielectric strength (kV)	60.45± 0.05 30.61	50–	IEC 60156
Viscosity (mm²/s)	20.29	36.8	ASTM D445
Acidity (mg KOH/g oil)	4.73	10.5	AOCS CD 3d - 63
Density at 20 °C (gm⁻³)	890	913	ASTM D 1298
Iodine Value (g/I₂/100g oil)	101.86	–	AOCS CD 1c - 85

a) Experimental value;   b) Iha et al (2014);   – Not reported

Similarly, the average linear correlation coefficient R^2 value increased in the following order:

Power law model → parabolic diffusion model → Elovich's model → Hyperbolic Model → Pseudo second order

Therefore, Pseudo second order model, having the highest average value of R^2, the lowest average RMS and SEE values, as well as the second lowest average AARD % value, was chosen as the best model that describes the extraction kinetics under investigation. Hence, in ascending order, the models that gave a good fit were Elovich's, hyperbolic and pseudo second order models.

Physicochemical properties of TCKO

The oil yield of TCK was 60.45 ± 0.05 % (in mass), which was higher than the value reported for other oil seeds such as cottonseed [44] and soybean [45] at 65 °C. This result indicates the potentials for industrial applications of TCKO. *Iha et al.* [3], Dos *Santos et al.* [4] and Monnet et al, [23], reported 50 % (in mass), 49 % (in mass) and 58.61 ± 0.13 %, respectively, for the TCK obtained from Brazil's coastal region, Brazil's Northeastern coastal region and Cô te d' Ivoire, respectively. These values were lower than those obtained in this report. This difference in the oil yield could be as a result of factors such as geographical location, variety, harvest period and post-harvest handling method [18].

Some important physicochemical properties of TCK oil were presented in Table 3. These properties were evaluated and compared with those reported by *Iha et al.* [3]. In Table 3, the viscosity and acidity of TCKO[a] differ significantly from that of TCKO[b], with the later having higher viscosity and acidity than the former. This relatively low viscosity and acid value of TCKO[b] could be due to differences in species/breed as well as variation

in the climatic regions where *Terminalia catappa L* was grown. Hence, an improved breed of TCK enhances its yield and oil properties. The iodine value (IV) of the TCKO in this work was higher than 83.92 g/I₂/100g oil reported by Dos santos et al, [4]. This shows the high level of saturation of the oil as indicated by its fatty acid profile. The Dielectric Strength (DS) value of TCKO was 30.61 kV. This value was found to be lower than that of soya bean oil (39 kV) [46] but higher than the DS of palm kernel oil (25 kV) [46]. The DS value of TCKO could be improved with further purification and transesterification to obtain TCKO based transformer fluid. The introduction of natural antioxidant additives would help to further improve the DS and other physicochemical properties of TCKO.

FT-IR analyses of TCK oil

Fig. 6 Shows the FTIR spectrum of TCKO. The result was analyzed and compared with the known signature of identified materials using the FT-IR library [47]. The spectrum showed 6 discernable peaks at frequency range of 4000 to 200 cm⁻¹. The peak ranges centered at 3474.88 cm⁻¹ and 3305.14 cm⁻¹ are characteristics of O–H stretching which is an indication of the presence of water. The peak centered at 2929.00 cm⁻¹ was characteristics of C – H stretching which showed the presence of fats and carbohydrates. Conversely, the peak centered at 2868.24 cm⁻¹ was characteristics of C = H stretching which showed the presence oxygen-containing compounds (Aldehydes and Ketones). Furthermore, the peak at 2344.55 cm⁻¹ was characteristics of N – H stretching, associated with amine species, as could be confirmed by the presence of Nitrogen. Finally, the peak at 2036.90 cm⁻¹ was characteristics of O – H stretching, hence indicated the presence of organic molecules and compounds. The presence of C–H and O–H linked to fats/oil indicated the potentials for utilization
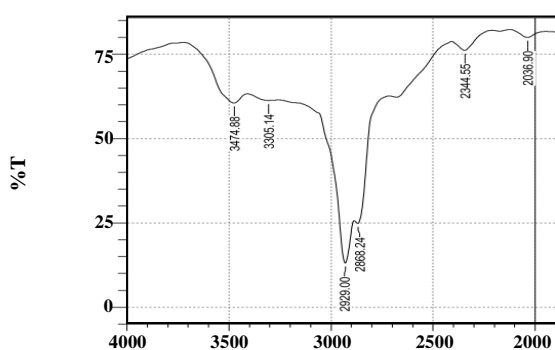
Fig. 6: FT-IR spectrum of TCKO.

of TKCO as transformer fluid. Also the following groups: C–H, C=H, N–H, and O–H found in TCKO indicated biodegradability of the oil. However, the uncertainties associated with the FT-IR spectra result has been identified and they include; uncertainty due to bandwidth effect, systematic effects associated with the test lamp calibration (e.g. spectral mismatch, spatial variation, detector linearity and lamp current settling) and random effect associated with test lamp calibration (e.g. measurement noise, lamp current stability and room temperature effect).

CONCLUSIONS

The *Terminalia catappa* Kernel Oil (TCKO) extraction has been found to follow the initial fast washing and late slow diffusion actions. Temperature and particle size significantly influenced the kinetics of the extraction process as well as the oil yield. The experimental and the calculated oil yield values for the pseudo second order, hyperbolic and Elovich's models were well correlated, whereas those of power law and parabolic diffusion models significantly disagreed. Among the five kinetics models, three (hyperbolic, Elovich's and pseudo second order models) fitted adequately to the experimental data while two (parabolic and power law models) did not. The very good fitting of best fit models (hyperbolic, Elovich's and pseudo second order), to the experimental data was attributed to their predominant diffusion rate. The pseudo second order model gave the best fit. The pysicochemical properties and FT-IR result of the TCKO showed its potential for industrial application as transformer oil. The FT-IR of TCKO contains C – H, C = H, N – H, and O – H functional groups,

indicating the presence of water, organic molecules, and compounds that ensure biodegradability of the oil.

Nomenclature

AARD	Average Absolute Relative Deviation
ASTM	American Society for Testing and Material
A.O.A.C	Association of Official Analytical Chemist
A.O.C.S	American Oil Chemist's Society
IEC	International Electrotechnical commission
TC	*Terminalia catappa*
TCK	*Terminalia catappa* kernel
TCKO	*Terminalia catappa* kernel oil
DS	Dielectric strength
RMS	Root mean square
SEE	Standard Error of Estimation

REFERENCES

[1] Masjuki H.H., Maleque M.A., Kubo A., Nonaka T., Palm Oil and Mineral Oil based Lubricants. Their Tribological and Emission Performance, *Tribology International*, **32**: 305 – 314 (1999).

[2] Wan Nick W.B., Ani F.N., Masjuki H.H. Eng Giap S.G., Rheology of Bio-Edible Oils According to Several Rheological Models and Its Potential as Hydraulic Fluid, *Industrial Crops and Products*, **22**: 249-255 (2005).

[3] Iha O.K., Alves F.C.S., Suarez P.A.Z., Silva Cassia R.P., Meneghetti M.R., Meneghetti S.M.P., Potential Application of Terminalia Catappa L. and Carapa Guianensis Oils for Biofuel Production: Physical-Chemical Properties of Neat Vegetable Oils, Their Methylesters and Bio-Oils (hydrocarbons), *Industrial Crops and Products*, **52**: 95-98 (2014).

[4] Dos Santos I.C.F., de Carvalho S.H.V., Solleti J.I., Ferreira dela Sellas W., Teixeira da Silva de La Salles K., Meneghetti S.M.P., Studies of Terminalia Catappa L. oil: Characterization and Biodiesel Production, *Journal of Bioresource Technology*, **99**: 6545-6549 (2008).

[5] Likozar B., Pohar A., Levec J., Transesterification of Oil to Biodiesel in a Continuous Tubular Reactor with Static Mixers: Modelling Reaction Kinetics, Mass Transfer, Scale-up and Optimization Considering Fatty Acid Composition, *Fuel Processing Technology*, **142**: 326-336 (2016).

[6] Likozar B., Levec J., Transesterification of Canola, Palm, Peanut, Soybean and Sunflower Oil with Methanol, Ethanol, Isopropanol, Butanol and Tert-Butanol to Biodiesel: Modelling of Chemical Equilibrium, Reaction Kinetics and Mass Transfer Based on Fatty Acid Composition, *Applied Energy*, **123**: 108-120 (2014).

[7] Likozar B., Levec J., Effect of Process Conditions on Equilibrium, Reaction Kinetics and Mass Transfer for Triglyceride Transesterification to Biodiesel: Experimental and Modeling based on Fatty Acid Composition, *Fuel Processing Technology*, **122**: 30-41 (2014).

[8] Abdelmalik A.A., Chemically Modified Palm Kernel Oil Ester: A Possible Sustainable Alternative Insulating Fluid, *Sustainable Materials and Technologies*, **1–2**: 42 – 51 (2014).

[9] Agu C., Menkiti M., Kadurumba C., Menkiti N., Process Parameter Optimization for Transformer Oil Extraction from Terminalia Catappa Seed Using Response Surface Methodology, *Journal of the Chinese Advanced Materials Society*, **3**(4): 328-344 (2015).

[10] Cermak S.C., Brandon K.B., Isbell T.A., Synthesis and Physical Properties of Estolides from Lesquerella and Castor Fatty Acid Esters, *Industrial Crops and Products*, **23**: 54-64 (2006).

[11] Wang L., Weller C.L., Recent Advances in the Extraction of Nutraceuticals from Plants, *Trends in Food Science and Technology*, **17**: 300-312 (2006).

[12] Azmir J., Zaidul I.S.M., Rahman M.M., Sharif K.M., Mohamed A., Sahena F., Omar A.K.M., Techniques for Extraction of Bioactive Compounds from Plant Materials: A Review, *Journal of Food Engineering*, **117**: 426-245 (2013).

[13] Atabani A.E., Silitonga A.S., Ong H.C., Mahlia T.M.I., Masjuki H.M., Badruddin I.A., Fayaz H., Non-Edible Vegetable Oils: A Critical Evaluation of Oil Extraction, Fatty Acid Compositions, Biodiesel Production, Characteristics, Engine Performance and Emissions Production. Renew, Sustain, *Energy Rev.*, **18**: 211 – 245 (2013).

[14] Angela M., Meireles A., "Extracting Bioactive Compunds for Food Products. Theory and Application", CRC Press, Taylor & Francis group. 600 Broken Sound Parkway NW, Suite 300, Boca Raton, FL 33487-2742 London New York, (2009).

[15] Shi J., Mazza G., In: Le Maguer (Eds.), "Functional Foods: Biochemical and Processing Aspects", Vol. II, Functional Foods and Nutraceuticals Series, CRC Press Inc., *Boca Raton*, 331– 366 (2002).

[16] Kitanovic S., Milenovic D., Veeljkovic V.B., Empirical Kinetic Models for the resinoid extraction from aerial parts of St John's Wort (Hypericum Perforatum L.) *Journal of Biochemical Engineering*, **41**: 1-11 (2008).

[17] Pestana V.R., Zambiazi R.C., Mendonca C.R.B., Bruscatto M.H., Lerma-Garcia M.J., Ramis Ramos G., Quality Changes and Tocopherols and γ- Oryzanol Concentrations in RBO During the Refining Process, *Journal of the American Oil Chemists' Society*, **85**: 1013-1019 (2008).

[18] Menkiti C.M., Agu C.M., Udeigwe T.K., Extraction of Oil from *Terminalia catappa L.*: Process Parameter Impacts, Kinetics, and Thermodynamics, *Industrial Crops and Products*, **77**: 713-723 (2015).

[19] Devappa R.K., Makkar H.P.S., Becker K., Optimization of Conditions for the Extraction of Phorbol Esters from Jatropha Oil, *Biomass and Bioenergy*, **34**: 1125-1133 (2010).

[20] Fernandez C.M., Ramos M.J. Perez A., Rodriguez J.F., Production of Biodiesel from Winery Waste: Extraction, Refining and Transesterification of Grape Seed Oil, *Bioresource Technology*, **101**: 7019 – 7024(2010).

[21] Sulaiman S., Abdul Aziz A.R., Arova M.K., Optimization and Modeling of Extraction of Solid Coconut Waste Oil, *Journal of Food Engineering*, **114**: 228 – 234 (2013).

[22] Navarro Cerutti M.L.M., Ulson de Souza A.A., Ulsos de Souza S.M.A., Solvent Extraction of Vegetable Oils: Numerical and Experimental Study, *Food and Bioproducts Processing*, **90**: 199 – 204 (2012).

[23] Monnet Y.T., Gbogeuri A., Kouadio P., Koffi B., Kouame L.P., Chemical Characterization of Seeds and Seed oil from mature *Terminalia catappa* fruits harvested in Cote d'Ivoire, *International Journal of Biosciences*, **10**: 110-124 (2012).

[24] Lin C.C., Chen Y.L., Lin J.M., Ujiie T., Evaluation of the Antioxidant and Hepatoprotective Activity of Terminalia Catappa, *American Journal of Chinese Medicine*, **25** (2): 153-161(1997).

[25] Masuda T., Yonemori S., Oyama Y., Tekeda Y., Tanaka T., Andoh T., Shinohara A., Nakata M., Evaluation of the Antioxidant Activity of Environmental Plants: Activity of the Leaf Extracts from Seashore Plants, *Journal of Agricultural and Food Chemistry*, **47**: 1749-1754 (1999).

[26] Lin C.C., Hsu Y.F., Lin T.C., Effects of Punicalagin and Punicalin on Carrageenan Induced Inflammation in Rats, *American Journal of Chinese Medicine*, **27**: 371 – 376 (1999).

[27] Chen P.S., Li J.H., Liu T.Y., Lin T.C., Folk Medicine Terminalia Catappa and Its Major Tannin Component, Punicalagin, are Effective Against Bleomycin-Induced Genotoxicity in Chinese Hamster Ovary Cells, *Cancer Lett*, **152** (2): 115-122 (2000).

[28] Fan Y.M., Xu L.Z., Gao J., Wang Y., Tang X.H., Zhao X.N., Zhang Z.X., Phytochemical and Anti-Inflammatory Studies on Terminalia Catappa, *Fitoterapia*, **75**: 253-260 (2004).

[29] Oliveria J.T.A., Vasconcelos I.M., Bezerra L.C.N.M., Silveira S.B., Monteiro A.C.O., Moreira R.A., Composition and Nutritional Properties of Seeds from Pachira Aquatic Aubl, Sterculia striata St Hil et Naud and Terminalia catappa Linn, *Food Chemistry*, **70**: 185 – 191 (2000).

[30] Agu C.M., Production, "Characterization and Utilization Potential of Bioextracts as Transformer Oil", M.Eng. Thesis. Department of Chemical Engineering, Faculty of Engineering, Nnamdi Azikiwe University, Awka, Anambra State, Nigeria, July (2014).

[31] Weerawatanakorn M., "*Terminalia catappa* Seeds Oil as a New Dietary Healthy Oil Source", *The Annual Meeting of the International Society for Nutraceuticals and Functional Foods (ISNFF)*, Taipei, Taiwan, (2013).

[32] Qu W., Pan Z., Ma H., Extraction Modeling and Activities of Antioxidants from Pomegranate Marc, *Journal of Food Engineering*, **99**: 16 – 23 (2010).

[33] Huang Z., Yang M.-J., Liu S.-F., Ma Q., Supercritical Carbon Dioxide Extraction of Baizhu: Experiments and Modeling, *The Journal of Supercritical Fluids*, **58**: 31 – 39 (2011).

[34] Alirezaei M., Zare D., Nassiri S.M., Application of Computer vision for Determining Viscoelastic Characteristics of Date Fruits, *Journal of Food Engineering*, **118**: 326 – 332 (2013).

[35] Meziane S., Kadi H., Kinetics and Thermodynamics of Oil Extraction from Olive Cake, *Journal of the American Oil Chemists' Society*, **85** (4): 391-396 (2008).

[36] Eikani M.H., Golmohammad F., Homani S.S., Extraction of Pomegranate (*Punica granatum L.)* Seed Oil Using Superheated Hexane, *Journal of Food and Bioproducts Processing*, **90**(1): 32 – 36 (2012).

[37] Wang L., Yang B., Du X., Yi C., Optimization of Supercritical Extraction of Flavonoids from *Pueraria lobata*, *Journal of Food Chemistry*, **108**: 737-741 (2008).

[38] Bimakar M., AbdulRaham R., Taip F.S., Ganjloo A., Md Salleh L., Selamat J., Hamid A., Zaidul I.S.M., Comparison of Different Extraction Methods for the Extraction of Major Bioactive Flavonoid Compounds from Spearmint (Mentha spicata L.) Leaves, *Journal of Food and Bioproducts Processing*, **89**: 67-72 (2011).

[39] Ozkal S.G., Yener M.E., Bayindirli L., Mass Transfer Modeling of Apricot Kernel Oil Extraction with Supercritical Carbon Dioxide, *Journal of Supercritical Fluids*, **35**: 119-127 (2005).

[40] Salgin U., Uysal B.Z., Calimli A., Supercritical Fluid Extraction of Jojoba Oil, *Journal of the American Oil Chemists' Society*, **81**: 293-296 (2004).

[41] Sayyar S., Abidin Z.Z., Yunus R., Muhammad. Extraction of Oil from Jatropha Seeds Optimization and Kinetics, *American Journal of Applied Sciences*, **6**(7): 1390 – 1395 (2009).

[42] Doker O., Salgin U., Yildiz N., Aydogmus M., Calimli A., Extraction of Sesame Seed Oil Using Supercritical Carbon Dioxide and Mathematical Modeling, *Journal of Food Engineering*, **97**: 360-366 (2010).

[43] Linares A.R., Hase S.L., Vergara M.L., Resnik S.L. Modeling Yerba Mate Aqueous Extraction Kinetics: Influence of Temperature, *Journal of Food Engineering*, **97**: 471 – 477 (2010).

[44] Khan N.U., Basal H., Hassan G., Cottonseed Oil Yield via Economic Heterosis and Heritability in Intraspecific Cotton Population, *African Journal of Biotechnology*, **9** (44): 7418–7428 (2010).

[45] Lawson O.S., Oyewumi A., Ologunagba F.O., Ojomo A.O., Evaluation of the Parameters Affecting the Solvent Extraction of Soybean Oil, ARPN *Journal of Engineering and Applied Sciences*, **5**(10): 51–55 (2010).

[46] Usman M.A., Olanipekun O.O., Henshaw U.T., A Comparative Study of Soya Bean Oil and Palm Kernel Oil as Alternatives to Transformer Oil, *Journal of Emerging Trends in Engineering and Applied Sciences*, **3**: 33-37(2012).

[47] Barbara S., "Analytical Techniques in Science. Infrared spectroscopy; Fundamentals and Application", John Wiley & Sons, Inc., London New York, (2004).

Supplementary Information

Table S1: Linearized Kinetic parameters for TC oil extraction at 35, 40, 45, 50 and 55°C

	35°C					40°C					45°C					50°C					55°C				
	0.5mm	1.0mm	1.5mm	2.0mm	2.5mm	0.5mm	1.0mm	1.5mm	2.0mm	2.5mm	0.5mm	1.0mm	1.5mm	2.0mm	2.5mm	0.5mm	1.0mm	1.5mm	2.0mm	2.5mm	0.5mm	1.0mm	1.5mm	2.0mm	2.5mm
Parabolic																									
A_0	5.92	14.84	14.03	14.55	11.79	7.75	16.78	16.07	15.57	14.04	9.25	18.34	19.36	19.41	15.86	12.05	21.48	19.71	20.56	18.87	14.88	23.07	22.10	23.20	21.91
A_1	3.908	2.276	2.137	1.901	1.980	3.899	2.293	2.107	2.005	1.976	4.004	2.310	1.990	1.800	2.011	3.907	2.144	2.163	1.878	1.868	3.826	2.252	2.104	1.825	1.776
R^2	0.990	0.890	0.898	0.836	0.837	0.982	0.875	0.854	0.846	0.820	0.981	0.908	0.859	0.824	0.856	0.983	0.847	0.900	0.860	0.855	0.983	0.877	0.898	0.851	0.802
RMS (%)	0.021	0.061	0.058	0.071	0.080	0.028	0.062	0.066	0.068	0.078	0.029	0.050	0.056	0.060	0.064	0.026	0.058	0.048	0.052	0.056	0.024	0.050	0.045	0.049	0.060
SEE	0.374	0.781	0.703	0.819	0.850	0.520	0.844	0.847	0.831	0.899	0.545	0.717	0.785	0.809	0.803	0.507	0.887	0.701	0.736	0.749	0.490	0.821	0.690	0.743	0.859
ARE %	0.101	0.481	0.438	0.614	0.787	0.161	0.474	0.544	0.551	0.728	0.170	0.321	0.384	0.431	0.519	0.128	0.407	0.296	0.335	0.375	0.101	0.319	0.257	0.291	0.421
SSE	4.19	18.30	14.82	20.13	21.68	8.11	21.36	21.54	20.73	24.26	8.91	15.41	18.51	19.65	19.36	7.71	23.62	14.76	16.26	16.83	7.19	20.24	14.28	16.57	22.12
HYBRID %	0.168	0.802	0.730	1.023	1.312	0.268	0.791	0.907	0.919	1.213	0.284	0.535	0.641	0.719	0.864	0.213	0.678	0.494	0.558	0.625	0.169	0.531	0.429	0.484	0.702
MPSED %	2.706	7.894	7.478	9.160	10.362	3.675	7.980	8.546	8.733	10.064	3.824	6.413	7.265	7.805	8.343	3.328	7.513	6.222	6.747	7.243	3.125	6.524	5.789	6.381	7.746
SD	0.0030	0.0144	0.0131	0.0184	0.0236	0.0048	0.0142	0.0163	0.0165	0.0218	0.0051	0.0096	0.0115	0.0129	0.0156	0.0038	0.0122	0.0089	0.0100	0.0113	0.0030	0.0096	0.0077	0.0087	0.0126

Research Article

Table S1: Continued

	35°C					40°C					45°C					50°C					55°C				
Power	0.5mm	1.0mm	1.5mm	2.0mm	2.5mm	0.5mm	1.0mm	1.5mm	2.0mm	2.5mm	0.5mm	1.0mm	1.5mm	2.0mm	2.5mm	0.5mm	1.0mm	1.5mm	2.0mm	2.5mm	0.5mm	1.0mm	1.5mm	2.0mm	2.5mm
B	22.27	24.72	23.31	22.87	20.49	24.13	26.76	25.28	24.33	22.74	26.10	28.32	28.05	27.29	24.65	28.49	30.88	29.08	28.74	27.05	30.96	32.85	31.22	31.19	29.75
n	0.217	0.122	0.115	0.101	0.105	0.216	0.123	0.113	0.107	0.105	0.221	0.125	0.107	0.096	0.108	0.216	0.114	0.117	0.101	0.100	0.212	0.121	0.113	0.097	0.094
R^2	0.967	0.815	0.823	0.754	0.750	0.952	0.799	0.772	0.767	0.733	0.948	0.838	0.779	0.742	0.775	0.951	0.762	0.828	0.783	0.771	0.953	0.802	0.826	0.767	0.713
RMS (%)	0.452	0.254	0.223	0.204	0.209	0.489	0.273	0.239	0.222	0.218	0.545	0.280	0.235	0.209	0.222	0.564	0.276	0.264	0.223	0.213	0.585	0.303	0.267	0.226	0.218
SEE	6.603	2.936	2.352	1.957	1.729	7.694	3.494	2.739	2.365	2.059	9.402	3.958	3.090	2.546	2.428	10.479	4.132	3.761	2.982	2.615	11.618	5.015	4.124	3.323	2.937
ARE %	42.12	20.56	16.84	13.68	11.36	46.63	23.38	19.05	16.64	14.42	53.35	25.40	20.39	17.13	17.05	56.31	25.28	23.96	19.49	17.71	59.19	28.93	25.04	20.62	18.83
SSE	1308	259	166	115	90	1776	366	225	168	127	2652	470	286	194	177	3294	512	424	267	205	4049	754	510	331	259
HYBRID %	70.20	34.27	28.07	22.80	18.93	77.72	38.96	31.74	27.73	24.04	88.91	42.33	33.98	28.55	28.41	93.84	42.14	39.93	32.48	29.52	98.64	48.21	41.73	34.37	31.39
MPSED %	59.05	32.92	28.89	26.34	27.02	64.23	35.43	31.03	28.66	28.13	72.17	36.57	30.63	27.05	28.74	75.10	36.16	34.37	28.94	27.62	78.19	39.93	34.99	29.56	28.3241
SD	1.2636	0.6169	0.5052	0.4105	0.3407	1.3989	0.7013	0.5714	0.4991	0.4327	1.6004	0.7620	0.6117	0.5140	0.5114	1.6892	0.75585	0.7187	0.5847	0.5313	1.7756	0.8679	0.7512	0.6187	0.5650

Table S1: Continued

	35°C					40°C					45°C					50°C					55°C				
Hyperbolic	0.5mm	1.0mm	1.5mm	2.0mm	2.5mm	0.5mm	1.0mm	1.5mm	2.0mm	2.5mm	0.5mm	1.0mm	1.5mm	2.0mm	2.5mm	0.5mm	1.0mm	1.5mm	2.0mm	2.5mm	0.5mm	1.0mm	1.5mm	2.0mm	2.5mm
C_1	1.470	1.688	1.613	1.572	1.271	1.588	1.881	1.763	1.703	1.486	1.721	2.138	2.199	2.184	1.746	1.969	2.413	2.301	2.392	2.138	2.234	2.690	2.632	2.762	2.488
C_2	0.022	0.034	0.034	0.035	0.029	0.023	0.036	0.036	0.036	0.033	0.024	0.040	0.045	0.047	0.037	0.028	0.045	0.044	0.049	0.045	0.031	0.048	0.049	0.055	0.051
R^2	0.988	0.982	0.986	0.963	0.966	0.989	0.977	0.972	0.965	0.960	0.991	0.988	0.975	0.959	0.973	0.988	0.975	0.989	0.973	0.978	0.985	0.979	0.989	0.979	0.958
RMS (%)	0.032	0.026	0.023	0.037	0.041	0.031	0.029	0.031	0.035	0.041	0.028	0.019	0.026	0.032	0.235	0.028	0.026	0.017	0.024	0.024	0.028	0.022	0.016	0.020	0.030
SEE	0.597	0.385	0.323	0.497	0.528	0.608	0.449	0.463	0.493	0.563	0.547	0.304	0.398	0.474	3.511	0.585	0.441	0.281	0.378	0.357	0.621	0.398	0.262	0.331	0.480
ARE %	0.006	0.006	0.154	0.182	0.157	0.438	0.196	0.095	0.048	0.083	0.625	0.133	0.152	0.128	24.418	0.113	0.150	0.163	0.069	0.207	0.174	0.071	0.136	0.168	0.184
SSE	10.68	4.44	3.13	7.40	8.37	11.10	6.04	6.43	7.28	9.51	8.97	2.78	4.76	6.74	369.81	10.26	5.83	2.37	4.28	3.82	11.55	4.76	2.07	3.29	6.92
HYBRID %	0.01	0.01	0.26	0.30	0.26	0.73	0.33	0.16	0.08	0.14	1.04	0.22	0.25	0.21	40.70	0.19	0.25	0.27	0.11	0.35	0.29	0.12	0.23	0.28	0.31
MPSED %	4.16	3.38	3.00	4.79	5.38	3.97	3.71	4.07	4.50	5.36	3.58	2.44	3.31	4.09	31.90	3.56	3.32	2.24	3.14	3.08	3.64	2.87	2.01	2.59	3.89
SD	0.0001	0.0002	0.0046	0.0055	0.0047	0.0088	0.0059	0.0019	0.0010	0.0025	0.0188	0.0040	0.0030	0.0026	0.7325	0.0023	0.0045	0.0049	0.0021	0.0062	0.0035	0.0014	0.0041	0.0050	0.0055

Table S1: Continued

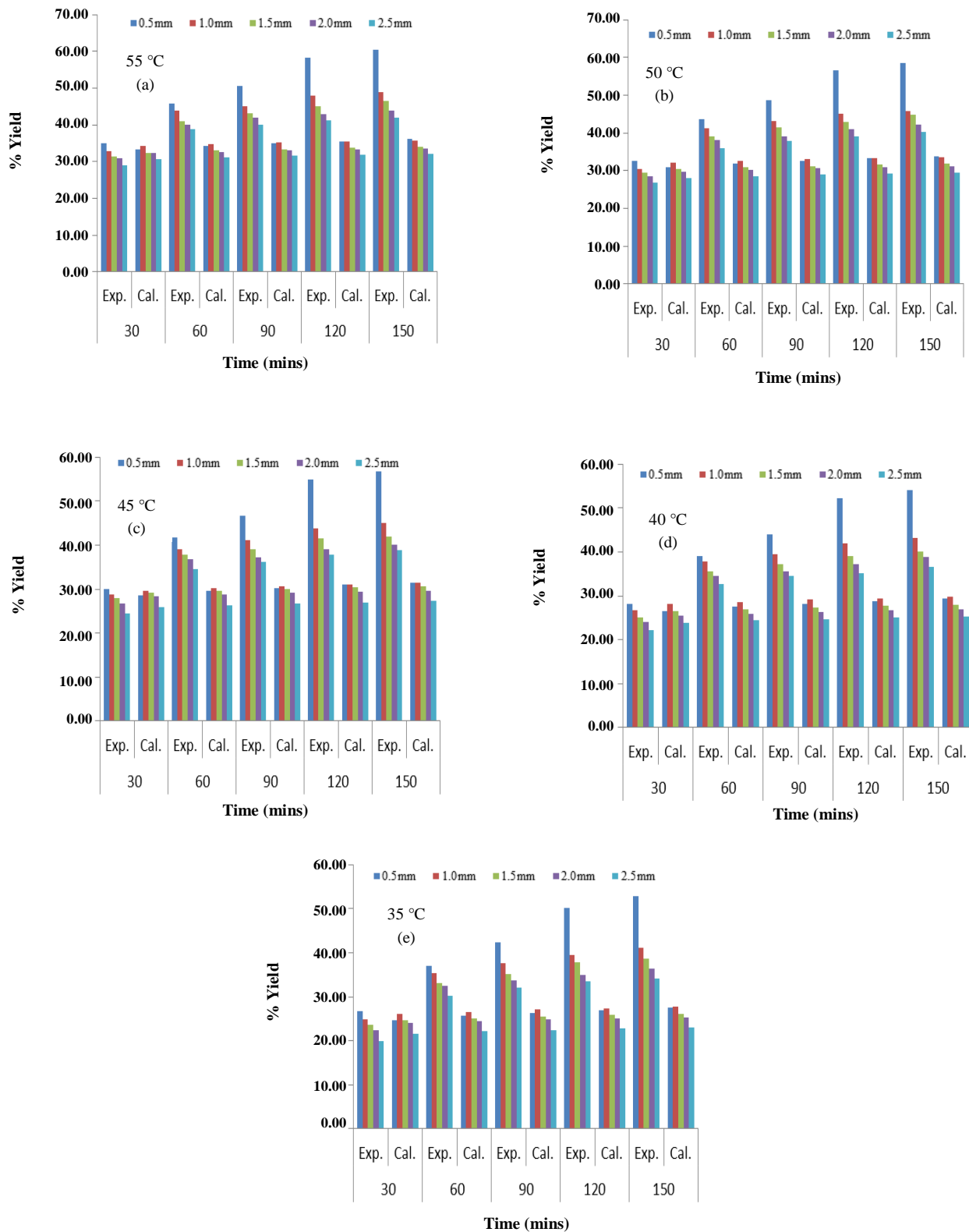|		35℃					40℃					45℃					50℃					55℃			
		0.5mm	1.0mm	1.5mm	2.0mm	2.5mm	0.5mm	1.0mm	1.5mm	2.0mm	2.5mm	0.5mm	1.0mm	1.5mm	2.0mm	2.5mm	0.5mm	1.0mm	1.5mm	2.0mm	2.5mm	0.5mm	1.0mm	1.5mm	2.0mm	2.5mm
Elovich's	E0	-29.52	-7.23	-6.64	-4.18	-7.81	-27.86	-5.54	-4.62	-4.10	-5.59	-27.45	-3.88	-0.12	1.65	-3.87	-23.70	0.34	-1.18	2.23	0.51	-20.10	1.20	1.78	5.23	4.18
	E_1	16.36	9.86	9.25	8.301	8.667	16.38	9.952	9.185	8.737	8.667	16.86	9.963	8.661	7.866	8.763	16.434	9.368	9.349	8.162	8.149	16.085	9.761	9.095	7.966	7.810
	R^2	0.987	0.949	0.955	0.907	0.912	0.985	0.937	0.923	0.914	0.897	0.988	0.960	0.925	0.895	0.924	0.988	0.919	0.956	0.924	0.925	0.988	0.937	0.954	0.922	0.882
	RMS (%)	0.026	0.040	0.037	0.051	0.057	0.025	0.042	0.046	0.049	0.057	0.021	0.032	0.040	0.045	0.045	0.020	0.041	0.031	0.037	0.039	0.019	0.035	0.029	0.035	0.045
	SEE	0.435	0.533	0.469	0.616	0.626	0.468	0.599	0.617	0.624	0.682	0.431	0.473	0.572	0.627	0.585	0.417	0.647	0.466	0.543	0.539	0.417	0.589	0.461	0.539	0.665
	ARE %	0.026	0.249	0.219	0.363	0.459	0.012	0.263	0.306	0.328	0.448	0.020	0.151	0.216	0.261	0.292	0.007	0.227	0.146	0.193	0.211	0.017	0.171	0.125	0.157	0.258
	SSE	5.674	8.531	6.590	11.402	11.762	6.572	10.774	11.433	11.666	13.952	5.569	6.704	9.815	11.798	10.251	5.229	12.554	6.523	8.843	8.727	5.207	10.401	6.369	8.727	13.257
	HYBRID%	0.043	0.415	0.364	0.606	0.765	0.021	0.439	0.510	0.547	0.747	0.033	0.252	0.361	0.436	0.486	0.011	0.378	0.243	0.322	0.352	0.029	0.284	0.208	0.261	0.429
	MPSED %	3.317	5.212	4.822	6.642	7.329	3.194	5.480	6.014	6.310	7.341	2.755	4.109	5.131	5.858	5.870	2.583	5.321	4.028	4.834	5.070	2.510	4.542	3.776	4.517	5.825
	SD	0.001	0.007	0.007	0.011	0.014	0.000	0.008	0.009	0.010	0.013	0.001	0.005	0.006	0.008	0.009	0.000	0.007	0.004	0.006	0.006	0.001	0.005	0.004	0.005	0.008

Fig. S1a to e: Comparison of experimental and the calculated yields using parabolic diffusion model for TCK oil extraction at different operation conditions.
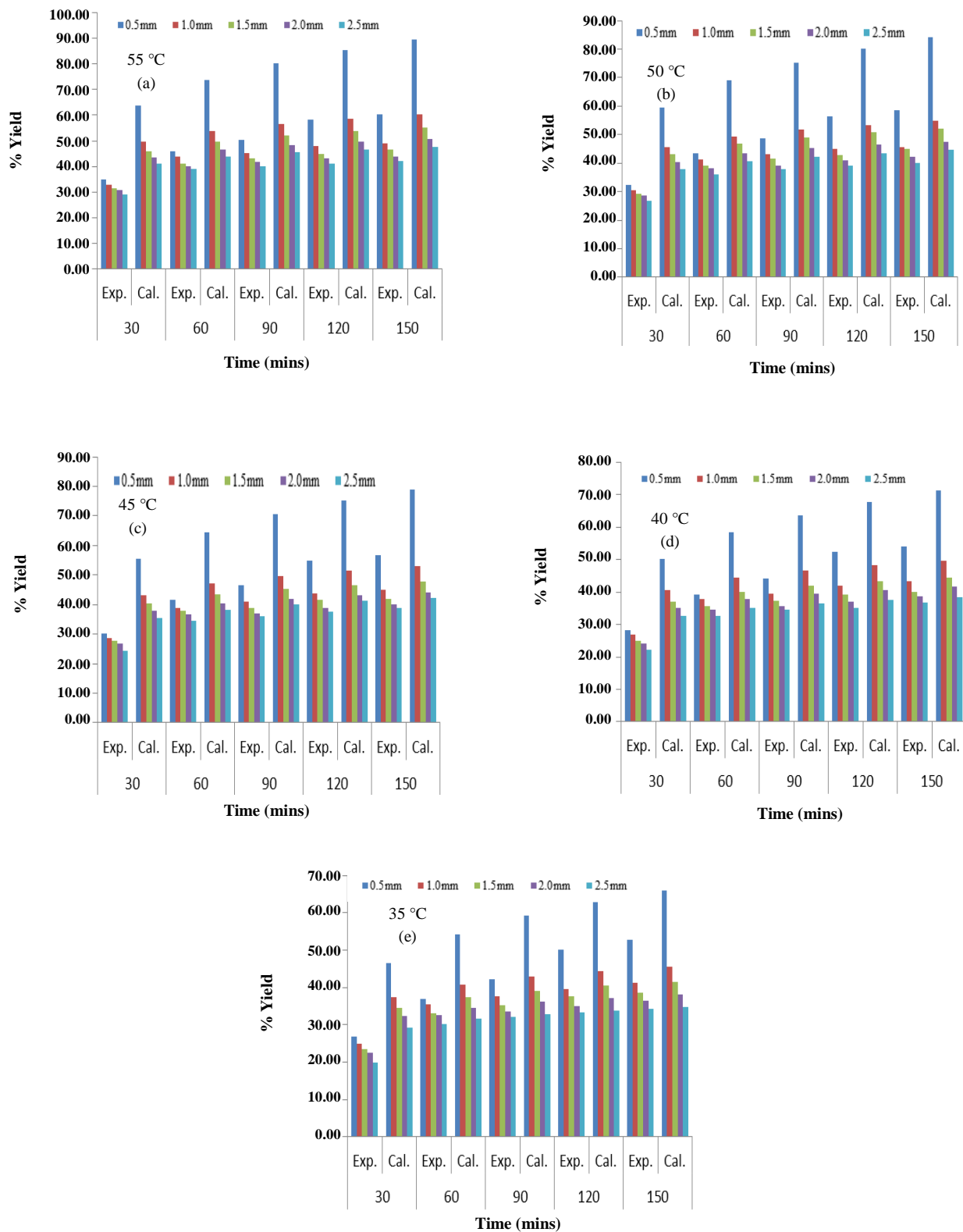
Fig. S2a to e: Comparison of experimental and the calculated yields using power law model for TCK oil extraction at different operation conditions.
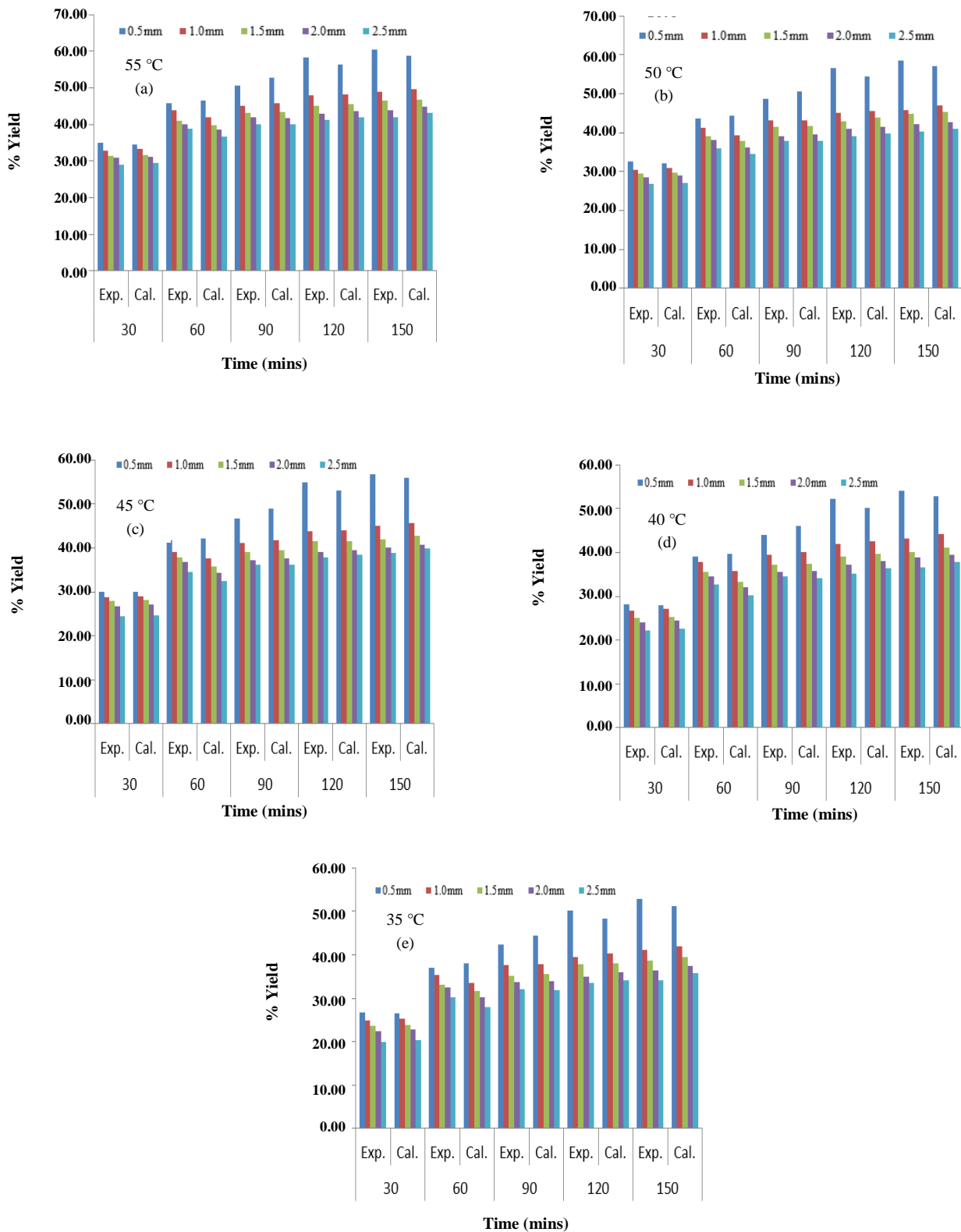
Fig. S3a to e: Comparison of experimental and the calculated yields using hyperbolic model for TCK oil extraction at different operation conditions.
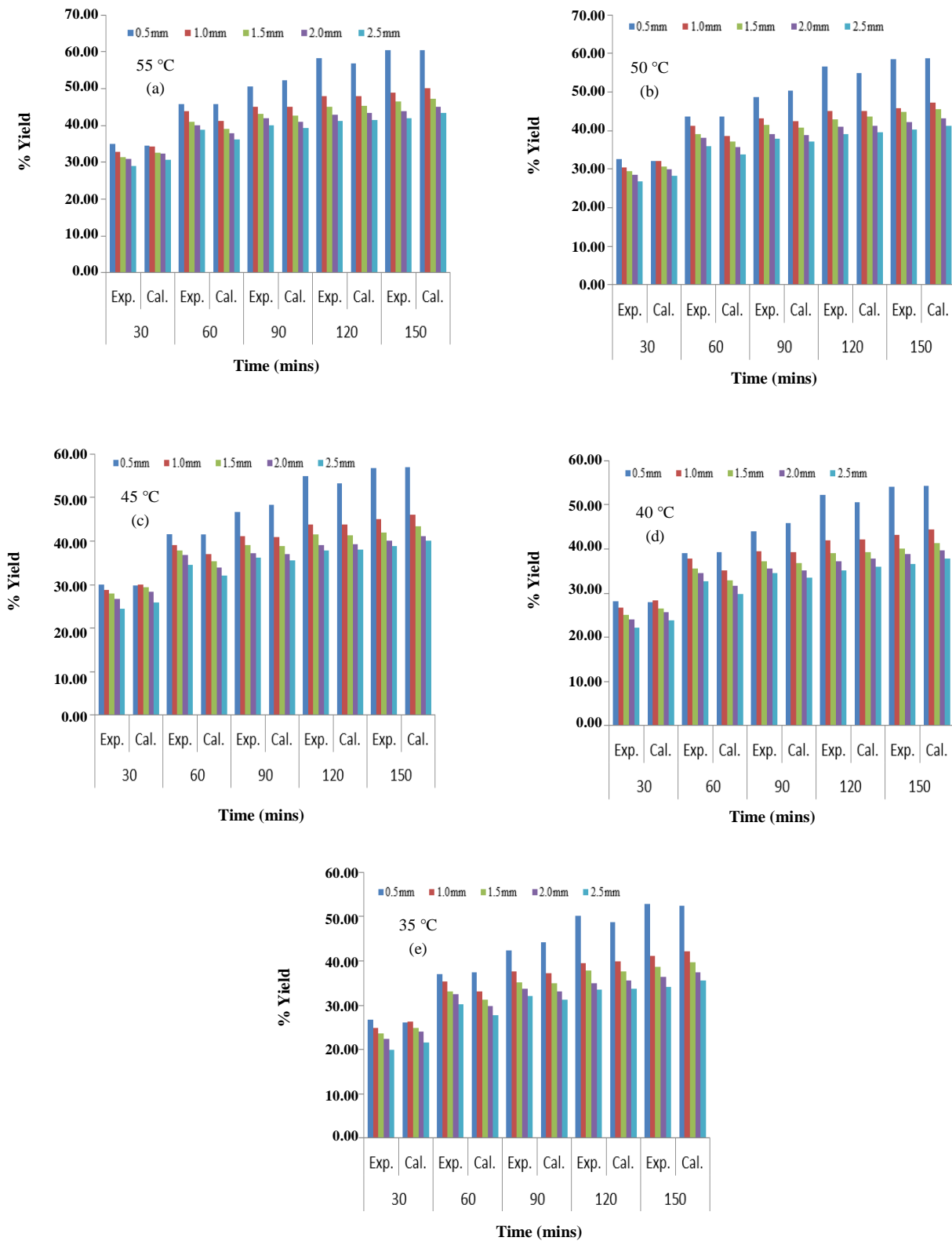
Fig. S4a to e: Comparison of experimental and the calculated yields using Elovich's model for TCK oil extraction at different operation conditions.